A refined FSDT for the static analysis of functionally graded sandwich plates

JL Mantari[+1], EV Granados[ϕ]

[+]Faculty of Mechanical Engineering, Universidad de Ingeniería y Tecnología, Av. Cascanueces 2221, Santa Anita, Lima, Perú.

[ϕ]Faculty of Mechanical Engineering, National University of Engineering, Av. Túpac Amaru 210, Rimac, Lima, Perú.

Abstract. This paper presents a static analysis of functionally graded plates (FGPs) by using a new first shear deformation theory (FSDT). This theory contains only four unknowns, with is even less than the classical FSDT. In this paper a simply supported FG square sandwich plate is subjected to a bi-sinusoidal load. The governing equations for static bending analysis are derived by employing the principle of virtual works. These equations are then solved via Navier-type, closed form solutions. The accuracy of the present theory is ascertained by comparing it with various available solutions in the literature.

---

[1]Corresponding Author email: jmantari@utec.edu.pe, tel: +00511 3540070; Cell: +0051 96224551;

Keywords: Shear deformation theory; FSDT; Static analysis; Functionally graded materials.

1. Introduction

Functionally graded materials (FGMs) can be defined as advanced materials having graded transition in mechanical properties, either continuous or in fine, discrete steps, across the interface. This material is produced by mixing two or more materials in a certain volume ratio (commonly ceramic and metal). FGMs have been proposed, developed and successfully used in industrial applications since 1980’s [1]. These materials were initially designed as a thermal barrier for aerospace structures and fusion reactors. They are now being developed for general use as structural components subjected to high temperatures.

The areas where FGM offer potential improvements and advantages in engineering applications include a reduction of in-plane and transverse through-the-thickness stresses, prevention or reduction of the delamination tendencies in laminated or sandwich structures, improved residual stress distribution, enhanced thermal properties, higher fracture toughness, and reduced stress intensity factors [2].

Several analytical and numerical formulations to model the behavior of single and multilayered structures are available in the literature. Among them, the classical first-order shear deformation theory (FSDT) based on Raissner and Mindlin, assume constant transverse shear stresses in the thickness direction, thus the theory need a shear correction factors to adjust for unrealistic variation of the shear strain/stress. Nguyen et al. [15] studied the shear correction factor for FGMs. The authors showed that the shear correction factor for FGMs are not the same as for homogeneous plates, in fact, they showed that the shear correction factor is as a function of the ratio between elastic moduli of constituents and of the distribution of materials through the models. In this paper, for simplicity purposes, the considered shear correction factors are as in the paper by Carrera et al. [5].

Researchers have investigated the behavior of functionally graded plates (FGPs) under mechanical loads using, mostly, both the classical FSDT and the higher-order shear deformation theories (HSDT). In this paper, relevant works on FGM based on the classical and modified FSDTs was reviewed and presented in what follows. Zenkour [3] studied the bending analysis of FGPs resting on elastic foundation using the refined sinusoidal shear deformation theory, FSDT results were also presented. Singha et al. [4] investigated the nonlinear behavior of FGPs using the finite element method based on the FSDT. The authors evaluated the shear correction factors employing the energy equivalence principle.

Carrera et al. [5] evaluated the effect of thickness stretching in functionally graded (FG) plates and shells by using Carrera's Unified Formulation (CUF), FSDT results were also presented. Valizadeh et al. [6] studied the FGPs using a non-uniform rational B-spline based on FEM. The plate kinematics is based on the FSDT. Thai and Choi [7] presented a simple FSDT with four unknowns for FG plate considering a division of the transverse displacement w into bending and shear parts. (i.e. $w = w_b + w_s$). Thai et al. [8] analyzed the FG sandwich plates composed of FG face sheets and an isotropic homogeneous core by using a FSDT with four unknowns.

In the present paper, the static analysis of FGPs is studied by using a new FSDT with four unknowns in which instead of derivative terms in the displacement field, integral terms are presented for the first time. Such displacement field, which can be further implemented in higher order shear deformation theories, may require new mathematical strategies to numerically solve the present theory due to its novelty. The simply supported FG plate and sandwich plate is subjected to a bi-sinusoidal load. The mechanical properties of the plates are assumed to vary in the thickness direction according to a power law distribution in terms of the volume fractions of the constituents. The governing equations of the FGPs are derived by employing the principle virtual works. These equations are then solved via Navier solution. The accuracy of the present code is verified by comparing it with other HSDTs. Although similar results as the classical FSDT are found, the reduced number unknowns of this theory play a key importance in the performance. Consequently, the numerical solution may be of paramount interest in future works.

2. Theoretical Formulation

The mathematical model was built to solve both: (A) functionally graded plates and (B) sandwich plates. The plates of uniform thickness “h”, length “a”, and width “b” are shown in Fig. 1. The rectangular Cartesian coordinate system x, y, z, has the plane z = 0, coinciding with the mid-surface of the plates.

2.1. Functionally graded plates

The material properties for the plate of type A (Fig. 1a) vary through the thickness with a power law distribution, which is given below (Fig. 2a):

$$P_{(z)} = (P_t - P_b)V_{(z)} + P_b \ ,$$

$$V_{(z)} = (\frac{z}{h} + \frac{1}{2})^p \ ,$$

$$-\frac{h}{2} \le z \le \frac{h}{2} \qquad \text{(1a-c)}$$

where P denotes the effective material property, P_t and P_b denote the property of the top (fully ceramic) and bottom (fully metal) faces of the plate, respectively, and "p" is the exponent that specifies the material variation profile through the thickness. The effective material properties of the plate, including Young's modulus, E, and shear modulus, G, vary according to Equations (1a, b), and Poisson ratio, "ν" is assumed to be constant.

In the plate of type B, the bottom skin is isotropic (fully metal) and the top skin is isotropic (fully ceramic). The core layer is graded from metal to ceramic so that there are no interfaces between core and skins (see Fig. 1b).

The volume fraction in the core is obtained by adapting the power law distribution (Eq. 1b):

$$V_{(z)} = \left(\frac{z - h_1}{h_{core}} \right)^p ,$$

$$h_1 \le z \le h_2 \qquad \text{(2a-b)}$$

where h_{core} is the thickness of the core.

2.2. Displacement base field

The displacement field of the new theory is given as follows:

$$\begin{aligned} \bar{u}(x, y, z) &= u(x, y) - zk_1 \int \theta(x, y) dx, \\ \bar{v}(x, y, z) &= v(x, y) - zk_2 \int \theta(x, y) dy, \\ \bar{w}(x, y, z) &= w(x, y). \end{aligned} \qquad \text{(3a-c)}$$

where $u(x, y)$, $v(x, y)$, $w(x, y)$, and $\theta(x, y)$ are the four unknown displacement functions of middle surface of the plate. Note that the integrals do not have limits.

In the present paper is considered terms with integrals instead of terms with derivatives (see displacement field (3a-c) and [7]). Therefore, to find the values of the coefficients "k_1" and " k_2", similar procedure as in Thai and Choi [7] was performed obtaining:

$$\frac{k_1}{k_2} = \frac{\int \frac{\partial \theta}{\partial x} dy}{\int \frac{\partial \theta}{\partial y} dx} \tag{4}$$

2.3. Kinematic relations and constitutive relations

In the derivation of the necessary equations, small strains are assumed (i.e., displacements and rotations are small, and obey Hooke’s law). The linear strain expressions derived from the displacement model of Equations (3a-c), valid for thin, moderately thick and thick plate under consideration are as follows:

$$\varepsilon_{xx} = \varepsilon_{xx}^0 + z\varepsilon_{xx}^1,$$

$$\varepsilon_{yy} = \varepsilon_{yy}^0 + z\varepsilon_{yy}^1,$$

$$\varepsilon_{xy} = \varepsilon_{xy}^0 + z\varepsilon_{xy}^1,$$

$$\varepsilon_{xz} = \varepsilon_{xz}^0,$$

$$\varepsilon_{yz} = \varepsilon_{yz}^0. \tag{5a-e}$$

where

$$\varepsilon_{xx}^0 = \frac{\partial u}{\partial x}, \qquad \varepsilon_{xx}^1 = -\theta,$$

$$\varepsilon_{yy}^{0}=\frac{\partial v}{\partial y}, \qquad \varepsilon_{yy}^{1}=-\theta,$$

$$\varepsilon_{xy}^{0}=\frac{\partial v}{\partial x}+\frac{\partial u}{\partial y}, \qquad \varepsilon_{xy}^{1}=-\frac{\partial}{\partial y}\int\theta dx-\frac{\partial}{\partial x}\int\theta dy,$$

$$\varepsilon_{xz}^{0}=-\int\theta dx+\frac{\partial w}{\partial x}$$

$$\varepsilon_{yz}^{0}=-\int\theta dy+\frac{\partial w}{\partial y}, \qquad (6a\text{-}h)$$

The integrals appearing in the above expressions shall be resolved by a Navier type solution and can be expressed as follows:

$$\frac{\partial}{\partial y}\int\theta dx=A'\frac{\partial^{2}\theta}{\partial x\partial y}, \quad \frac{\partial}{\partial x}\int\theta dy=B'\frac{\partial^{2}\theta}{\partial x\partial y}, \quad \int\theta dx=A'\frac{\partial\theta}{\partial x}, \int\theta dy=B'\frac{\partial\theta}{\partial y}.$$

(7a-d)

where the coefficients "A'" and "B'" are defined according to the type of solution adopted, in this case via Navier. Therefore, "A'", "B'", k_1 and k_2 are expressed as follows:

$$A'=-\frac{1}{\alpha^{2}}, \qquad B'=-\frac{1}{\beta^{2}}, \qquad k_{1}=\alpha^{2}, \qquad k_{2}=\beta^{2}. \qquad (8a\text{-}d)$$

where α and β are defined in expressions (24a,b)

For the functionally graded plates, the stress–strain relationships can be expressed as:

$$\begin{Bmatrix}\sigma_{xx}\\ \sigma_{yy}\\ \tau_{xy}\\ \tau_{xz}\\ \tau_{yz}\end{Bmatrix}=\begin{bmatrix}Q_{11} & Q_{12} & 0 & 0 & 0\\ Q_{12} & Q_{22} & 0 & 0 & 0\\ 0 & 0 & Q_{66} & 0 & 0\\ 0 & 0 & 0 & Q_{55} & 0\\ 0 & 0 & 0 & 0 & Q_{44}\end{bmatrix}\begin{Bmatrix}\varepsilon_{xx}\\ \varepsilon_{yy}\\ \gamma_{xy}\\ \gamma_{xz}\\ \gamma_{yx}\end{Bmatrix}. \qquad (9)$$

in which, σ={ σ_{xx} , σ_{yy} , τ_{xy} , τ_{xz} , τ_{yz} }^{T} and ε={ ε_{xx} , ε_{yy} , γ_{xy} , γ_{xz} , γ_{yz} }^{T} are the stresses and the strain vectors with respect to the plate coordinate system. The Q_{ij} expressions in terms of engineering constants are given below:

$$Q_{11} = Q_{22} = \frac{E}{1-\nu^2}, \quad Q_{12} = \nu Q_{11}, \quad Q_{44} = Q_{55} = Q_{66} = \frac{E}{2(1+\nu)}. \tag{10a-c}$$

2.4. Principle of virtual works

The principle of virtual works of the considered FGPs is expressed as:

$$\delta U + \delta V = 0 \tag{11}$$

where δU is the virtual strain energy and δV is the external virtual works due to an external load q applied to the plate. Them can be written as:

$$\delta U = \int_V \left[\sigma_{xx}\delta\varepsilon_{xx} + \sigma_{yy}\delta\varepsilon_{yy} + \tau_{xy}\delta\gamma_{xy} + \tau_{xz}\delta\gamma_{xz} + \tau_{yz}\delta\gamma_{yz}\right]dV \tag{12}$$

$$\delta V = -\int_\Omega q\delta w d\Omega \tag{13}$$

Substituting the Equations (12), (13) into the Equation (11), the following integral equation can be obtained:

$$\int_\Omega \left(\int_{-h/2}^{+h/2} \left[\sigma_{xx}\delta\varepsilon_{xx} + \sigma_{yy}\delta\varepsilon_{yy} + \tau_{xy}\delta\gamma_{xy} + \tau_{xz}\delta\gamma_{xz} + \tau_{yz}\delta\gamma_{yz}\right]dz\right)d\Omega - \int_\Omega q\delta w d\Omega = 0 \tag{14}$$

$$\begin{aligned}&\int_\Omega (N_1\delta\varepsilon^0_{xx} + M_1\delta\varepsilon^1_{xx} + N_2\delta\varepsilon^0_{yy} + M_2\delta\varepsilon^1_{yy} + N_6\delta\gamma^0_{xy} + M_6\delta\gamma^1_{xy} + \\ &N_5\delta\gamma^0_{xz} + N_4\delta\gamma^0_{yz} - q\delta\overline{w})dxdy = 0\end{aligned} \tag{15}$$

where N_i and M_i are the resultants of the following integrations:

$$N_i = \int_{-h/2}^{+h/2} \sigma_i \, dz \,, \qquad \text{(i=1,2,6)}$$

$$N_i = \int_{-h/2}^{+h/2} K\sigma_i \, dz \,, \qquad \text{(i=4,5)}$$

$$M_i = \int_{-h/2}^{+h/2} z\sigma_i \, dz \,, \qquad \text{(i=1,2,6)} \qquad \text{(16a-c)}$$

where K is the shear correction factor.

2.5. Plate governing equations

Using the displacement–strain relations (Equations 5a-e and 6a-h) and stress–strain relations (Equation 9), and applying integrating by parts and the fundamental lemma of variational calculus and collecting the coefficients of $\delta u, \delta v, \delta w, \delta\theta$ in Equation 15, the governing equations are obtained as:

$$\delta u : \frac{\partial N_1}{\partial x} + \frac{\partial N_6}{\partial y} = 0 \,,$$

$$\delta v : \frac{\partial N_2}{\partial y} + \frac{\partial N_6}{\partial x} = 0 \,,$$

$$\delta w : \frac{\partial N_5}{\partial x} + \frac{\partial^2 N_4}{\partial y} = -q \,,$$

$$\delta\theta : k_1 A' \frac{\partial^2 M_1}{\partial x^2} + k_2 B' \frac{\partial^2 M_2}{\partial y^2} + (k_1 A' + k_2 B') \frac{\partial^2 M_6}{\partial x \partial y} - k_1 A' \frac{\partial N_5}{\partial x} - k_2 B' \frac{\partial N_4}{\partial y} = 0 \qquad \text{(17a-d)}$$

By substituting the stress-strain relations into the definitions of force and moment resultants of the present theory given in Equation (16a-c) the following constitutive equations are obtained:

$$\mathrm{N_i} = \mathrm{A_{ij}} \varepsilon_j^0 + B_{ij} \varepsilon_j^1 \,, \qquad \text{(i=1,2,6)}$$

$$N_i = KA_{ij}\varepsilon_j^0 + KB_{ij}\varepsilon_j^1, \qquad (i=4,5)$$

$$M_i = B_{ij}\varepsilon_j^0 + C_{ij}\varepsilon_j^1, \qquad (i=1,2,6) \qquad (18a\text{-}c)$$

where

$$A_{ij} = \int_{-h/2}^{h/2} Q_{ij(z)}dz$$
$$B_{ij} = \int_{-h/2}^{h/2} zQ_{ij(z)}dz \qquad (19a\text{-}c)$$
$$C_{ij} = \int_{-h/2}^{h/2} z^2Q_{ij(z)}dz$$

From Equations (18a-c), it can be noticed that for N_i, and M_i the variables depending on x and y are the strains, ε_j^b (b=0,…,5). Therefore, the expressions in each of the plate governing equations (17a-d), for example $\frac{\partial N_i}{\partial x}$, $\frac{\partial M_i}{\partial x}$, can be expressed as follows:

$$\frac{\partial(N_i, M_i)}{\partial x} = (A_{ij},B_{ij})\begin{bmatrix} -\alpha^2 & 0 & 0 & 0 \\ 0 & -\alpha\beta & 0 & 0 \\ -\alpha\beta & -\alpha^2 & 0 & 0 \\ 0 & 0 & -\alpha^2 & k_1A'\alpha^2 \\ 0 & 0 & \alpha\beta & -k_2B'\alpha\beta \end{bmatrix}\begin{bmatrix} U_{mn} \\ V_{mn} \\ W_{mn} \\ \Theta_{mn} \end{bmatrix} +$$

$$(B_{ij},C_{ij})\begin{bmatrix} 0 & 0 & 0 & k_1A'\alpha^3 \\ 0 & 0 & 0 & k_2B'\alpha\beta^2 \\ 0 & 0 & 0 & (k_1A'+k_2B')\alpha^2\beta \\ 0 & 0 & 0 & 0 \\ 0 & 0 & 0 & 0 \end{bmatrix}\begin{bmatrix} U_{mn} \\ V_{mn} \\ W_{mn} \\ \Theta_{mn} \end{bmatrix} \qquad (20)$$

The elements of the 5x4 matrices are the coefficients obtained after taking the first derivation of the strains expression in the Equations (18a-c). As is known, the strains are expressed as a function of the 4 unknowns, described in Equations (3a-c). These unknowns are expressed as shown in the Equations (23a-d) in order to satisfy the simply supported boundary conditions.

The 5x4 matrices associated with $\frac{\partial M_i}{\partial x}$ in Equations 20, is called $\overline{M}_x^{1,b}$ (b=0,…,5). The symbols used in $\overline{M}_v^{a,b}$ are as follow: the first upper and lower (a,v) indicates the derivative (first derivative with respect to x, in the example), and the second upper character, b, indicates that the derivative is associates with the strain ε_j^b (b=0,…,5). Therefore, the expression $\frac{\partial^2 (N_i, M_i)}{\partial x \partial y}$, can be expressed as:

$$\frac{\partial^2 (N_i, M_i)}{\partial x \partial y} = (A_{ij}, B_{ij}) \overline{M}_{xy}^{2,0} + (B_{ij}, C_{ij}) \overline{M}_{xy}^{2,1}. \tag{21}$$

where, for example, $\overline{M}_{xy}^{2,0}$ is:

$$\overline{M}_{xy}^{2,0} = \begin{bmatrix} -\alpha^2\beta & 0 & 0 & 0 \\ 0 & -\alpha\beta^2 & 0 & 0 \\ \alpha\beta^2 & \alpha^2\beta & 0 & 0 \\ 0 & 0 & -\alpha^2\beta & k_1 A' \alpha^2 \beta \\ 0 & 0 & -\alpha\beta^2 & k_2 B' \alpha \beta^2 \end{bmatrix} \tag{22}$$

All matrices of type, $\overline{M}_v^{a,b}$, associated with the expressions of the plate governing Equations (17a-d) are given in the Appendix A.

3. Solution procedure

For the analytical solution of the partial differential equations (17a-d), the Navier method, based on double Fourier series, is used under the specified boundary conditions. Using Navier's procedure, the solution of the displacement variables satisfying the above boundary conditions can be expressed in the following Fourier series:

$$u(x,y) = \sum_{m=1}^{\infty} \sum_{n=1}^{\infty} U_{mn} \cos(\alpha x) \sin(\beta y), \qquad 0 \le x \le a;\ 0 \le y \le b \tag{23a}$$

$$v(x,y) = \sum_{m=1}^{\infty} \sum_{n=1}^{\infty} V_{mn} \sin(\alpha x) \cos(\beta y), \qquad 0 \le x \le a;\ 0 \le y \le b \tag{23b}$$

$$w(x,y)=\sum_{m=1}^{\infty}\sum_{n=1}^{\infty}W_{mn}\sin(\alpha x)\sin(\beta y),\qquad 0\le x\le a;\ 0\le y\le b \tag{23c}$$

$$\theta(x,y)=\sum_{m=1}^{\infty}\sum_{n=1}^{\infty}\Theta_{mn}\sin(\alpha x)\sin(\beta y),\qquad 0\le x\le a;\ 0\le y\le b \tag{23d}$$

where

$$\alpha=\frac{m\pi}{a},\ \beta=\frac{n\pi}{b}. \tag{24a,b}$$

Substituting Equations (23a-d) into Equations (17a-d), the following equations are obtained,

$$K_{ij}\Delta_j=F_j \qquad (i,j=1,......,5)\ \text{and}\ (K_{ij}=K_{ji}). \tag{25}$$

Elements of K_{ij} in Equation (25) can be obtained by using the matrices $\overline{M}_{v}^{a,b}$, and the governing equations (17a-d).

$$\{\Delta_j\}^T=\{U_{mn}\ V_{mn}\ W_{mn}\ \Theta_{mn}\}, \tag{26a}$$

$$\{F_j\}^T=\{0\quad 0\quad -Q'_{mn}\quad 0\} \tag{26b}$$

where Q'_{mn} are the coefficients in the double Fourier expansion of the transverse load,

$$q(x,y)=\sum_{m=1}^{\infty}\sum_{n=1}^{\infty}Q'_{mn}\sin(\alpha x)\sin(\beta y) \tag{27}$$

4. Numerical results and discussions

In this section the accuracy of the present FSDT which has a displacement field containing four unknowns, is evaluated. Numerical examples for static analysis of FG square plates with various indexes that specify the material variation profile through the thickness and several values of the side-to-thickness ratio “a/h” is also presented. Typical mechanical properties for metal and ceramics used in the FGPs are listed in Table 1. In the calculations, both, FGPs and FG sandwich plates are studied; also an analysis of the parameters was performed. For this study the following relations for presentations of non-dimensional deflection and non-dimensional stresses was utilized:

$$\bar{w} = w(\frac{a}{2}, \frac{b}{2}, z)\frac{10h^3E_t}{q_0a^4}, \qquad \bar{\sigma}_{xx} = \sigma_{xx}(\frac{a}{2}, \frac{b}{2}, z)\frac{h}{q_0a}, \qquad \bar{\sigma}_{xz} = \sigma_{xz}(0, \frac{b}{2}, z)\frac{h}{q_0a},$$

$$\bar{\sigma}_{xy} = \sigma_{xy}(0,0,z)\frac{h}{q_0a}, \qquad \bar{z} = \frac{z}{h}.$$

(28a-e)

4.1 Analysis of functionally graded plates

In this example problem, an FG square plate of type A is considered. The materials making up the plate are aluminum at the bottom, and alumina at the top face (see materials properties in Table 1). The simply supported square plate is subjected to a bi-sinusoidal load in the top face.

Table 2 presents the results of non-dimensional deflection $\bar{w}$ and normal stress $\bar{\sigma}_{xx}$ for various values of the side-to-thickness ratio a/h = {4, 10, 100} and index p = {0, 0.5, 1, 4, 10}. These results are compared with the quasi-3D solutions [5,10,12,14], HSDTs [9,14], and FSDT [13]. From this table can be noticed that values of deflection and normal stress obtained by the present theory are in good agreement with the quasi-3D solutions. It is also observed that the degree of accuracy of the results depends on the used shear correction factor for thick plates, as expected. In some cases K=1 is desirable (a/h=4, p≤1), but in other cases K=5/6. For large values of the side-to-thickness ratio "a/h" the influence of the shear correction factor decreases significantly. The values of the non-dimensional normal stresses $\bar{\sigma}_{xx}$ do not depend of the used shear correction factor, see Table 2.

4.2 Analysis of functionally graded sandwich plates

In this example, a simply supported FG square sandwich plate (B type) of thickness “h” will be analyzed. The bottom skin is aluminum with thickness h_b = 0.1h and the top skin is alumina with thickness h_t = 0.1h. The core is a FGM with mechanical properties changing according to Equation (2a). This sandwich plate is subjected to a bi-sinusoidal load in the top face.

Table 3 presents the results of non-dimensional deflection $\bar{w}$ and shear stress $\bar{\sigma}_{xz}$ for various values of the side-to-thickness ratio “a/h” and index “p”. These results are compared with the quasi-3D solutions [5,11,12,14], HSDTs [14], and FSDT [13]. From this table can be noticed that values of deflection and normal stress obtained by the present theory are in good agreement with the quasi-3D solutions. When the shear correction factor is neglected, i.e. K = 1 and $p \leq 1$, the deflection results by the present theory is close to the solutions proposed by Neves et al. [14]. As in the previous example, the influence of the shear correction factor decreases as the side-to-thickness ratio "a/h" increases. In the case of transverse shear stresses the shear correction factor K = 5/6 produce results closer to quasi-3D solutions than when K=1.

Table 4 presents results of non-dimensional in-plane shear stress $\bar{\sigma}_{xy}$ for side-to-thickness ratio a/h = {4, 100} and different index p = {0, 0.5, 1, 5, 10}. These results are also compared with quasi-3D solutions [11,12]. From this table can be noticed that the values of the non-dimensional in-plane shear stress $\bar{\sigma}_{xy}$ do not depend on the shear correction factor, i.e. K=1 can be used. In general, the present results are in agreement with the other solution presented in Table 4.

4.3 Parameter studies

Figure 3a shows the variation of non-dimensional deflection of FG square plate (A type) with side-to-thickness ratio a/h=5 as function of the index “*p*”. In this figure can be seen that when the shear correction factor is K=5/6, the results of this theory are very close to the solutions of the classical FSDT. For small values of the index "p", the three curves tend to approach each other.

Figure 3b shows the variation of non-dimensional deflection $\bar{w}$ of FG square sandwich plates (B type) with side-to-thickness ratio a/h=5 as a function of the index “*p*”. This figure shows that for large values of the index "p", the deflections depend on K but have almost a constant value. For a given geometry and considering the same materials that make up the two types of plates (A, B), the deflection values for a sandwich plate is lower than for a simple plate. This is because the sandwich plate is stiffer than the single FG plate due to its larger amount of metal, which contributes to the mechanical responses.

In Figure 4a, the variation of non-dimensional deflection $\bar{w}$ of FG square plate (A type) as a function of the side-to-thickness ratio "a/h" is shown. From this figure can be seen that for a given value of the side-to-thickness ratio "a/h", higher values of index “p” produces higher deflections. The three curves show the same trend and practically give the same values of deflection.

Figure 4b shows the variation of non-dimensional deflection $\bar{w}$ of FG square sandwich plate (B type) as a function of the side-to-thickness ratio "a/h". The curves of this graph follow the same trends as the curves of Figure 4b for a simple plate. Then, similar comments are valid.

The present non-dimensional stresses ($\bar{\sigma}_{xx}$, $\bar{\sigma}_{xy}$ and $\bar{\sigma}_{xz}$) distributions through the thickness of FG plate (type A) with a shear correction factor K={1, 5/6} along with the solutions provided by classical FSDT are shown in Figure 5a-c. From Figure 5c can be demonstrated, as it is well-known, that the shear correction factor K=5/6 is important for the transverse shear stress $\bar{\sigma}_{xz}$ results.

4.4 Conclusions

This paper presents a static analysis for FG single and sandwich plates using an original FSDT with 4 unknowns. The governing equations are obtained through the principle virtual works. These equations are solved via Navier’s method. The results were compared with the solutions of several theories. It is concluded that the results of the present theory with shear correction factor K=5/6 has a good agreement with quasi-3D theories for the static analysis. The shear correction factor has not clear influence in the deflections but strong influence on the transverse shear stress.

Acknowledgment

The first author wants to dedicate this work to his courageous daughter “Cielo”.

Appendix A: Definition of Constants in Equation (25)

Calculation of N, M and P:

$$\begin{bmatrix}(N_1, M_1)\\(N_2, M_2)\\(N_6, M_6)\end{bmatrix} = (\text{Aij,Bij})\begin{bmatrix}-\alpha & 0 & 0 & 0\\0 & -\beta & 0 & 0\\\beta & \alpha & 0 & 0\end{bmatrix} +$$

$$(\text{Bij,Cij})\begin{bmatrix}0 & 0 & 0 & k_1 A'\alpha^2\\0 & 0 & 0 & k_2 B'\beta^2\\0 & 0 & 0 & -(k_1 A' + k_2 B')\alpha\beta\end{bmatrix} \qquad \text{(A1)}$$

where i, j = 1, 2, 6

First derivative of N and M with respect to x:

$$\begin{bmatrix}\frac{\partial(N_1, M_1)}{\partial x}\\\frac{\partial(N_2, M_2)}{\partial x}\\\frac{\partial(N_6, M_6)}{\partial x}\end{bmatrix} = (\text{Aij,Bij})\begin{bmatrix}-\alpha^2 & 0 & 0 & 0\\0 & -\alpha\beta & 0 & 0\\-\alpha\beta & -\alpha^2 & 0 & 0\end{bmatrix} +$$

$$(\text{Bij,Cij})\begin{bmatrix}0 & 0 & 0 & k_1 A'\alpha^3\\0 & 0 & 0 & k_2 B'\alpha\beta^2\\0 & 0 & 0 & (k_1 A' + k_2 B')\alpha^2\beta\end{bmatrix} \qquad \text{(A2)}$$

First derivative of N and M with respect to y:

$$\begin{bmatrix} \dfrac{\partial(N_1, M_1)}{\partial y} \\ \dfrac{\partial(N_2, M_2)}{\partial y} \\ \dfrac{\partial(N_6, M_6)}{\partial y} \end{bmatrix} = (\text{Aij,Bij})\begin{bmatrix} -\alpha\beta & 0 & 0 & 0 \\ 0 & -\beta^2 & 0 & 0 \\ -\beta^2 & -\alpha\beta & 0 & 0 \end{bmatrix} +$$

$$(\text{Bij,Cij})\begin{bmatrix} 0 & 0 & 0 & k_1 A'\alpha^2\beta \\ 0 & 0 & 0 & k_2 B'\beta^3 \\ 0 & 0 & 0 & (k_1 A' + k_2 B')\alpha\beta^2 \end{bmatrix} \quad \text{(A3)}$$

Second partial derivative of N and M with respect to x:

$$\begin{bmatrix} \dfrac{\partial^2(N_1, M_1)}{\partial x^2} \\ \dfrac{\partial^2(N_2, M_2^c)}{\partial x^2} \\ \dfrac{\partial^2(N_6, M_6)}{\partial x^2} \end{bmatrix} = (\text{Aij,Bij})\begin{bmatrix} \alpha^3 & 0 & 0 & 0 \\ 0 & \alpha^2\beta & 0 & 0 \\ -\alpha^2\beta & -\alpha^3 & 0 & 0 \end{bmatrix} +$$

$$(\text{Bij,Cij})\begin{bmatrix} 0 & 0 & 0 & -k_1 A'\alpha^4 \\ 0 & 0 & 0 & -k_2 B'\alpha^2\beta^2 \\ 0 & 0 & 0 & (k_1 A' + k_2 B')\alpha^3\beta \end{bmatrix} \quad \text{(A4)}$$

Second partial derivative of N and M with respect to y:

$$\begin{bmatrix} \dfrac{\partial^2(N_1, M_1)}{\partial y^2} \\ \dfrac{\partial^2(N_2, M_2^c)}{\partial y^2} \\ \dfrac{\partial^2(N_6, M_6)}{\partial y^2} \end{bmatrix} = (\text{Aij,Bij})\begin{bmatrix} \alpha\beta^2 & 0 & 0 & 0 \\ 0 & \beta^3 & 0 & 0 \\ -\beta^3 & -\alpha\beta^2 & 0 & 0 \end{bmatrix} +$$

$$(Bij,Cij)\begin{bmatrix} 0 & 0 & 0 & -k_1A'\alpha^2\beta^2 \\ 0 & 0 & 0 & -k_2B'\beta^4 \\ 0 & 0 & 0 & (k_1A'+k_2B')\alpha\beta^3 \end{bmatrix} \qquad (A5)$$

Second partial derivative of N and M with respect to x and y:

$$\begin{bmatrix} \frac{\partial^2(N_1,M_1)}{\partial x\partial y} \\ \frac{\partial^2(N_2,M_2^c)}{\partial x\partial y} \\ \frac{\partial^2(N_6,M_6)}{\partial x\partial y} \end{bmatrix} = (Aij,Bij)\begin{bmatrix} -\alpha^2\beta & 0 & 0 & 0 \\ 0 & -\alpha\beta^2 & 0 & 0 \\ \alpha\beta^2 & \alpha^2\beta & 0 & 0 \end{bmatrix} +$$

$$(Bij,Cij)\begin{bmatrix} 0 & 0 & 0 & k_1A'\alpha^3\beta \\ 0 & 0 & 0 & k_2B'\alpha\beta^3 \\ 0 & 0 & 0 & -(k_1A'+k_2B')\alpha^2\beta^2 \end{bmatrix} \qquad (A6)$$

Example to get K(1,j), in Equation (25):

From the Equations A1 and A2, $\frac{\partial N_1}{\partial x}$ and $\frac{\partial N_6}{\partial y}$ can be easily obtained and substituted in Equation A7.

$$K(1,j) = \frac{\partial N_1^c}{\partial x} + \frac{\partial N_6^c}{\partial y}, \text{ where } j=1,2,\ldots,5. \qquad (A7)$$

Following the same technique the coefficients associated with Q and K can be obtained.

References

1. Koizumi M. The concept of FGM Ceramic transactions, Funct. Grad. Mater. 1993;34:3-10.
2. Birman V, Keil T, Hosder S. Functionally graded materials in engineering. In: Thomopoulus S, Birman V, Genin GM, editors. Structural Interfaces and Attachments in Biology. New York: Springer Science+Business Media New York, 2013. p. 19-41.
3. Zenkour AM. The refined sinusoidal theory for FGM plates on elastic foundations. Int J Mech Sci 2009;51:869-80.
4. Singha MK, Prakash T, Ganapathi M. Finite element analysis of functionally graded plates under transverse load. Finite Elem Anal Des 2011;47:453-60.
5. Carrera E, Brischetto S, Cinefra M, Soave M. Effects of thickness stretching in functionally graded plates and shells. Compos Part B: Eng 2011;42:123–33.
6. Valizadeh N, Natarajan S, Gonzalez OA, Rabczuk T, Bui TQ, Bordas SPA. NURBS-based finite element analysis of functionally graded plates: Static bending, vibration, buckling and flutter. Compos Struct 2013;99:309-26.
7. Thai HT, Choi DH. A simple first-order shear deformation theory for the bending and free vibration analysis of functionally graded plates. Compos Struct 2013;101:332-40.
8. Thai HT, Nguyen TK, Vo TP, Lee J. Analysis of functionally graded sandwich plates using a new first-order shear deformation theory. Eur J Mech – A/Solid 2014;45:211-25.
9. Zenkour AM. Generalized shear deformation theory for bending analysis of functionally graded plates. Appl Math Modell 2006;30:67–84.
10. Carrera E, Brischetto S, Robaldo A. Variable kinematic model for the analysis of functionally graded material plates. AIAA J 2008;46:194–203.
11. Brischetto S. Classical and mixed advanced models for sandwich plates embedding functionally graded cores. J Mech Mater Struct 2009;4:13–33.
12. Neves AMA, Ferreira AJM, Carrera E, Roque CMC, Cinefra M, Jorge RMN, et al. A quasi-3d sinusoidal shear deformation theory for the static and free vibration analysis of functionally graded plates. Compos Part B: Eng 2012;43:711–25.

13. Thai HT, Choi DH. A simple first-order shear deformation theory for the bending and free vibration analysis of functionally graded plates. Compos Struct 2013;101:332-40.

14. Neves AMA, Ferreira AJM, Carrera E, Cinefra M, Roque CMC, Jorge RMN, et al. Static, free vibration and buckling analysis of isotropic and sandwich functionally graded plates using a quasi-3D higher-order shear deformation theory and a meshless technique. Compos Part B: Eng 2013;44(1):657–74.

15. Nguyen TK, Sab K, Bonnet G. First-order shear deformation plate models for functionally graded materials. Composite Structures 2008;83:25–36.

Table Legends

Table 1. Material properties of the used FG plate.

Table 2. Dimensionless normal stress $\bar{\sigma}_{xx}$ and deflection $\bar{w}$ of Al/Al_2O_3 square plates under sinusoidal loads.

Table 3. Dimensionless shear stress $\bar{\sigma}_{xz}$ and deflection $\bar{w}$ of sandwich square plates embedding an Al/Al_2O_3 core under sinusoidal loads.

Table 4. Dimensionless shear stress $\bar{\sigma}_{xy}$ of sandwich square plate with FGM core (Al/Al2O3) under sinusoidal loads.

Figure Captions

Figure 1. Geometry of functionally graded plates.

Figure 2. Functionally graded function V_C along the thickness of an FG plate for different values of the index ‘‘p’’.

Figure 3. Variation of non-dimensional deflection $\bar{w}$ of FG square plates versus power law index “p” (a/h=5).

Figure 4. Variation of non-dimensional deflection $\bar{w}$ of FG square plates versus the side-to-thickness ratio “a/h” (p = {1, 5, 10}).

Figure 5. Variation of non-dimensional stresses through the thickness of FG square plates (p=5, a/h=10).

TABLES

Table 1.

Material	Properties	
	E (GPa)	**ν**
Aluminum (Al)	70	0.3
Alumina (Al_2O_3)	380	0.3

Table 2

p	Theory	ε_{zz}	$\bar{\sigma}_{xx}(h/3)$			$\bar{w}(0)$		
			a/h=4	**a/h=10**	**a/h=100**	**a/h=4**	**a/h=10**	**a/h=100**
0	Ref. [14]	0	0.5151	1.3124	13.1610	0.3786	0.2961	0.2803
	Ref. [14]	≠0	0.5278	1.3176	13.1610	0.3665	0.2942	0.2803
	Present (K=1)	**0**	**0.5269**	**1.3172**	**13.1718**	**0.3626**	**0.2934**	**0.2804**
	Present (K=5/6)	**0**	**0.5269**	**1.3172**	**13.1718**	**0.3790**	**0.2961**	**0.2804**
0.5	Ref. [14]	0	0.5736	1.4629	14.6720	0.5699	0.4579	0.4365
	Ref. [14]	≠0	0.5860	1.4680	14.6730	0.5493	0.4548	0.4365
	Present (K=1)	**0**	**0.5858**	**1.4645**	**14.7180**	**0.5454**	**0.4504**	**0.4347**
	Present (K=5/6)	**0**	**0.5858**	**1.4645**	**14.7180**	**0.5680**	**0.4541**	**0.4347**
1	FSDT (K=5/6)	0	0.8060	2.0150	20.1500	0.7291	0.5889	0.5625
	Ref. [9]	0	1.4894	-	-	0.5889	-	-
	Ref. [13]	0	0.5987	1.4968	14.9683	0.7291	0.5890	0.5625
	Ref. [5] N = 4	≠0	0.6221	1.5064	14.9690	0.7171	0.5875	0.5625
	Ref. [10]	≠0	0.6221	1.5064	14.9690	0.7171	0.5875	0.5625
	Ref. [12]	≠0	0.5925	1.4945	14.9690	0.6997	0.5845	0.5624
	Ref. [14]	≠0	0.5911	1.4917	14.9450	0.7020	0.5868	0.5647
	Present (K=1)	**0**	**0.5987**	**1.4968**	**14.9683**	**0.7013**	**0.5845**	**0.5625**
	Present (K=5/6)	**0**	**0.5987**	**1.4968**	**14.9683**	**0.7291**	**0.5890**	**0.5625**
4	FSDT (K=5/6)	0	0.6420	1.6049	1.6049	1.1125	0.8736	0.8280
	Ref. [9]	0	1.1783	-	-	0.8651	-	-
	Ref. [13]	0	0.4769	1.1922	11.9222	1.1125	0.8736	0.8286
	Ref. [5] N = 4	≠0	0.4877	1.1971	11.9230	1.1585	0.8821	0.8286
	Ref. [10]	≠0	0.4877	1.1971	11.9230	1.1585	0.8821	0.8286
	Ref. [12]	≠0	0.4404	1.1783	11.9320	1.1178	0.8750	0.8286
	Ref. [14]	≠0	0.4330	1.1588	11.7370	1.1108	0.8700	0.8240
	Present (K=1)	**0**	**0.4769**	**1.1922**	**11.9217**	**1.0651**	**0.8661**	**0.8285**
	Present (K=5/6)	**0**	**0.4769**	**1.1922**	**11.9217**	**1.1125**	**0.8736**	**0.8286**
10	FSDT (K = 5/6)	0	0.4796	1.1990	11.9900	1.3178	0.9966	0.9360
	Ref. [9]	0	0.8775	-	-	1.0089	-	-
	Ref. [13]	0	0.3563	0.8907	8.9072	1.3178	0.9966	0.9361
	Ref. [5] N = 4	≠0	0.1478	0.8965	8.9077	1.3745	1.0072	0.9361
	Ref. [10]	≠0	0.3695	0.8965	8.9077	1.3745	1.0072	0.9361
	Ref. [12]	≠0	0.3227	1.1783	11.9320	1.3490	0.8750	0.8286
	Ref. [14]	≠0	0.3097	0.8462	8.6010	1.3334	0.9888	0.9227
	Present (K=1)	**0**	**0.3563**	**0.8907**	**8.9027**	**1.2541**	**0.9864**	**0.9355**
	Present (K=5/6)	**0**	**0.3563**	**0.8907**	**8.9027**	**1.3178**	**0.9966**	**0.9356**

Table 3

p	Theory	ε_{zz}	$\bar{\sigma}_{xz}(h/6)$			$\bar{w}(0)$		
			a/h=4	a/h=10	a/h=100	a/h=4	a/h=10	a/h=100
0	Ref. [14]	0	0.2193	0.2202	0.2202	0.4612	0.3736	0.3568
	Ref. [14]	≠0	0.2208	0.2227	0.2228	0.4447	0.3711	0.3568
	Present (K=1)	**0**	**0.1733**	**0.1733**	**0.1733**	**0.4474**	**0.3721**	**0.3579**
	Present (K=5/6)	**0**	**0.2080**	**0.2080**	**0.2080**	**0.4653**	**0.3750**	**0.3579**
0.5	Ref. [14]	0	0.2511	0.2522	0.2522	0.6422	0.5277	0.5058
	Ref. [14]	≠0	0.2546	0.2581	0.2585	0.6168	0.5238	0.5058
	Present (K=1)	**0**	**0.1977**	**0.1978**	**0.1978**	**0.6211**	**0.5231**	**0.5045**
	Present (K=5/6)	**0**	**0.2373**	**0.2373**	**0.2374**	**0.6446**	**0.5268**	**0.5045**
1	FSDT (K = 5/6)	0	0.2458	0.2458	0.2458	0.7738	0.6337	0.6073
	Ref. [13]	0	-	-	-	0.7406	0.6005	0.5740
	Ref. [5] N = 4	≠0	0.2604	0.2594	0.2593	0.7628	0.6324	0.6072
	Ref. [11]	≠0	0.2613	0.2605	0.2603	0.7628	0.6324	0.6072
	Ref. [12]	≠0	0.2742	0.2788	0.2793	0.7416	0.6305	0.6092
	Ref. [14]	≠0	0.2745	0.2789	0.2795	0.7417	0.6305	0.6092
	Present (K=1)	**0**	**0.2048**	**0.2048**	**0.2048**	**0.7461**	**0.6293**	**0.6073**
	Present (K=5/6)	**0**	**0.2458**	**0.2458**	**0.2458**	**0.7739**	**0.6337**	**0.6073**
4	FSDT (K = 5/6)	0	0.1877	0.1877	0.1877	1.0285	0.8191	0.7796
	Ref. [13]	0	-	-	-	1.0699	0.8407	0.7975
	Ref. [5] N = 4	≠0	0.2400	0.2398	0.2398	1.0930	0.8307	0.7797
	Ref. [11]	≠0	0.2429	0.2431	0.2432	1.0934	0.8321	0.7797
	Ref. [12]	≠0	0.2723	0.2778	0.2785	1.0391	0.8202	0.7784
	Ref. [14]	≠0	0.2696	0.2747	0.2753	1.0371	0.8199	0.7784
	Present (K=1)	**0**	**0.1564**	**0.1564**	**0.1564**	**0.9869**	**0.8124**	**0.7795**
	Present (K=5/6)	**0**	**0.1877**	**0.1877**	**0.1877**	**1.0285**	**0.8191**	**0.7796**
10	FSDT (K = 5/6)	0	0.1234	0.1234	0.1234	1.1109	0.8556	0.8075
	Ref. [13]	0	-	-	-	1.1841	0.8970	0.8429
	Ref. [5] N = 4	≠0	0.1932	0.1944	0.1946	1.2172	0.8740	0.8077
	Ref. [11]	≠0	0.1932	0.1944	0.1946	1.2172	0.8740	0.8077
	Ref. [12]	≠0	0.2016	0.2059	0.2064	1.1780	0.8650	0.8050
	Ref. [14]	≠0	0.1995	0.2034	0.2039	1.1752	0.8645	0.8050
	Present (K=1)	**0**	**0.1029**	**0.1029**	**0.1029**	**1.0601**	**0.8475**	**0.8073**
	Present (K=5/6)	**0**	**0.1234**	**0.1234**	**0.1234**	**1.1108**	**0.8556**	**0.8074**

Table 4

p	Theory	ε_{zz}	$\bar{\sigma}_{xy}\ (h/3)$	
			a/h=4	a/h=100
0	**Present (K=1)**	**0**	**0.3187**	**7.9684**
	Present (K=5/6)	**0**	**0.3187**	**7.9684**
0.5	**Present (K=1)**	**0**	**0.3414**	**8.5288**
	Present (K=5/6)	**0**	**0.3414**	**8.5288**
1	Ref. [11]	0	0.3007	8.4968
	Ref. [12]	0	0.3303	8.4882
	Ref. [11]	≠0	0.3007	8.4968
	Ref. [12]	≠0	0.3167	8.4911
	Present (K=1)	**0**	**0.3399**	**8.4984**
	Present (K=5/6)	**0**	**0.3399**	**8.4984**
5	Ref. [11]	0	0.1999	6.4942
	Ref. [12]	0	0.2317	6.4454
	Ref. [11]	≠0	0.1996	6.4942
	Ref. [12]	≠0	0.2248	6.4441
	Present (K=1)	**0**	**0.2598**	**6.4962**
	Present (K=5/6)	**0**	**0.2598**	**6.4962**
10	Ref. [11]	0	0.1412	5.1402
	Ref. [12]	0	0.1745	5.0745
	Ref. [11]	≠0	0.1403	5.1401
	Ref. [12]	≠0	0.1687	5.0754
	Present (K=1)	**0**	**0.2057**	**5.1414**
	Present (K=5/6)	**0**	**0.2057**	**5.1414**

Figures

Figure 1.

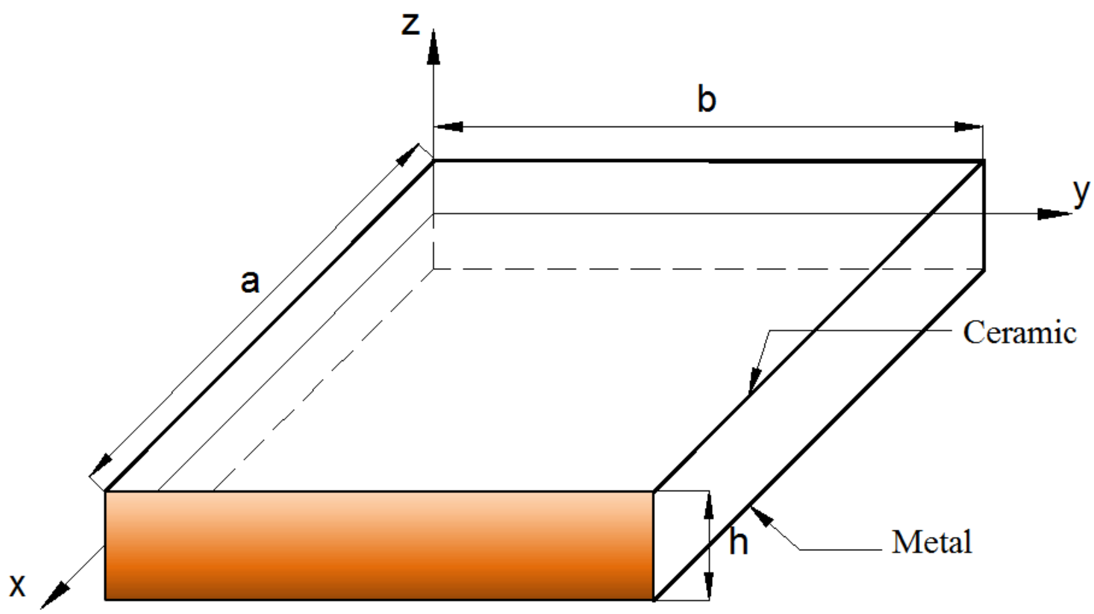

(a) FG plate

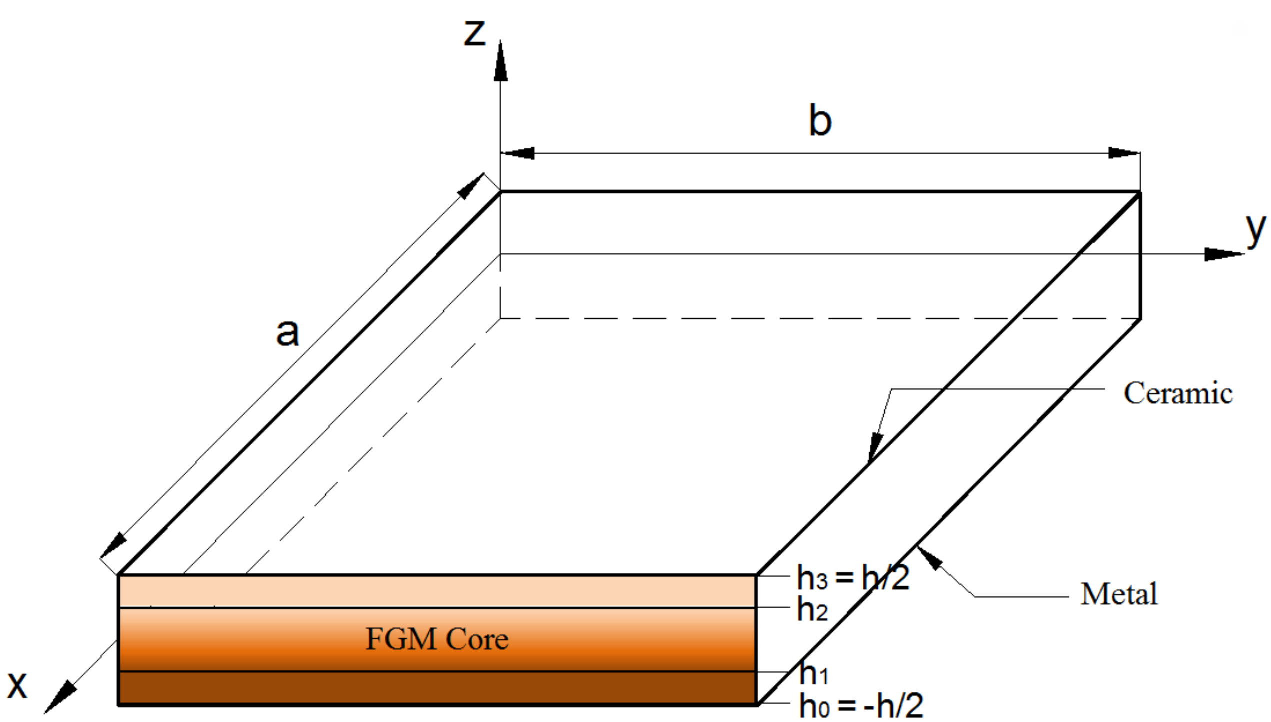

(b) Sandwich plate with an FG core and isotropic skins.

Figure 2.

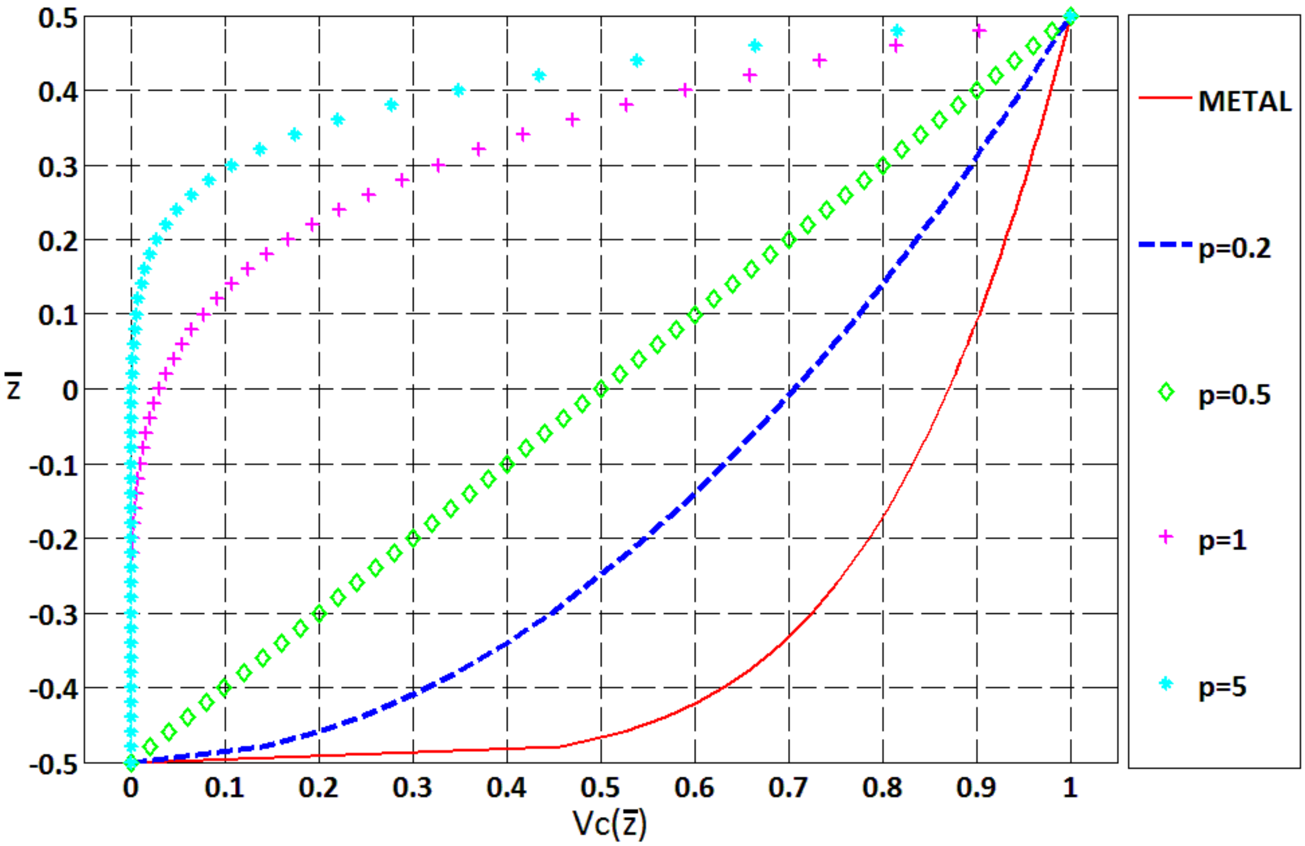

(a) FG plate

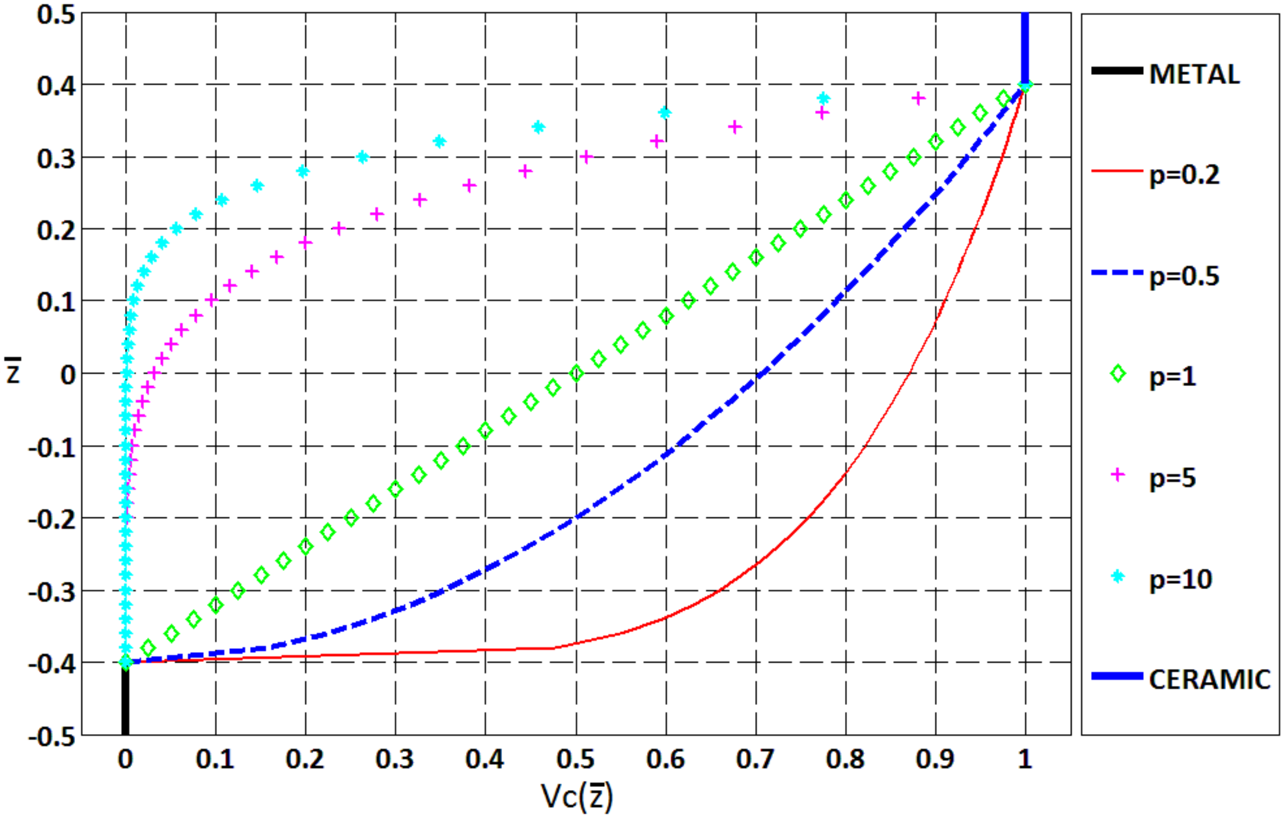

(b) Sandwich plate with an FG core and isotropic skins.

Figure 3.

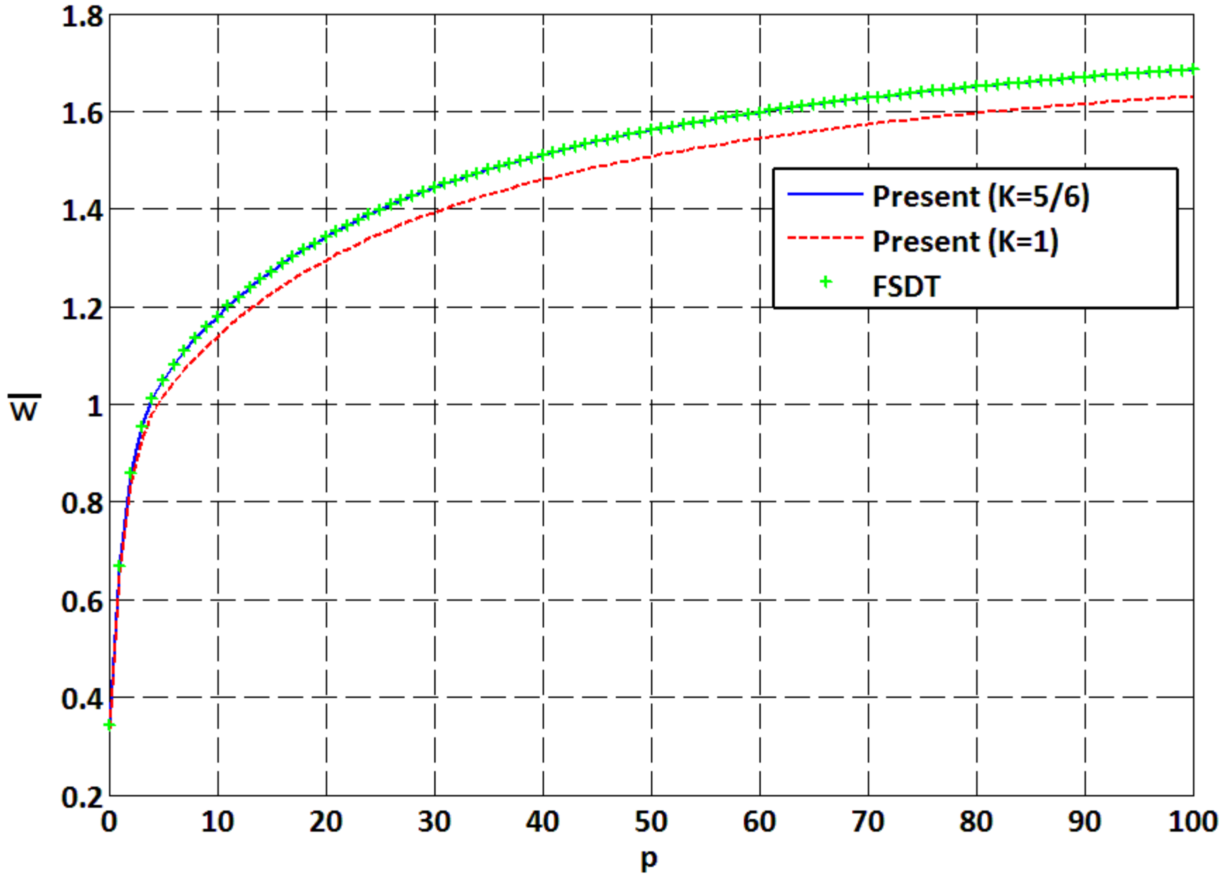

(a) FG plate

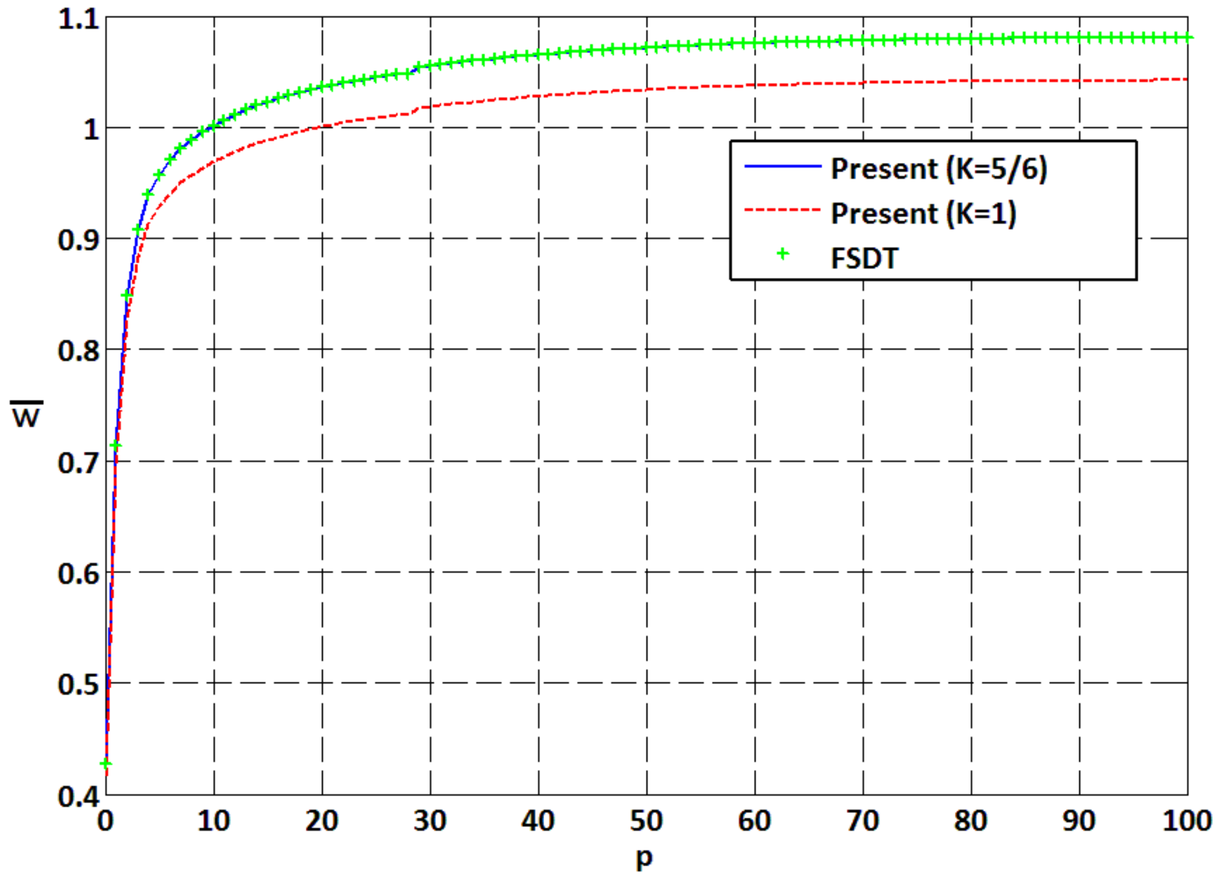

(b) Sandwich plate with an FG core and isotropic skins.

Figure 4.

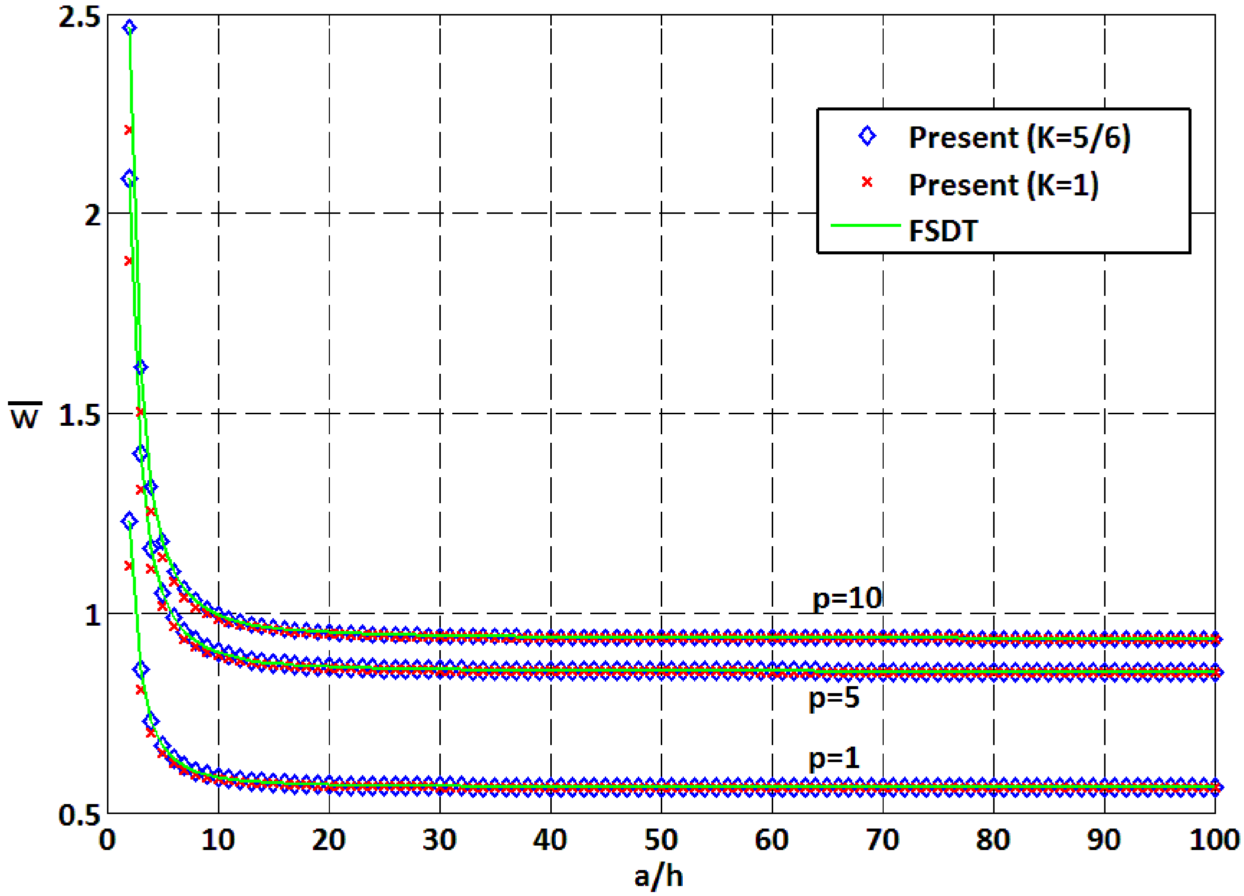

(a) FG plate

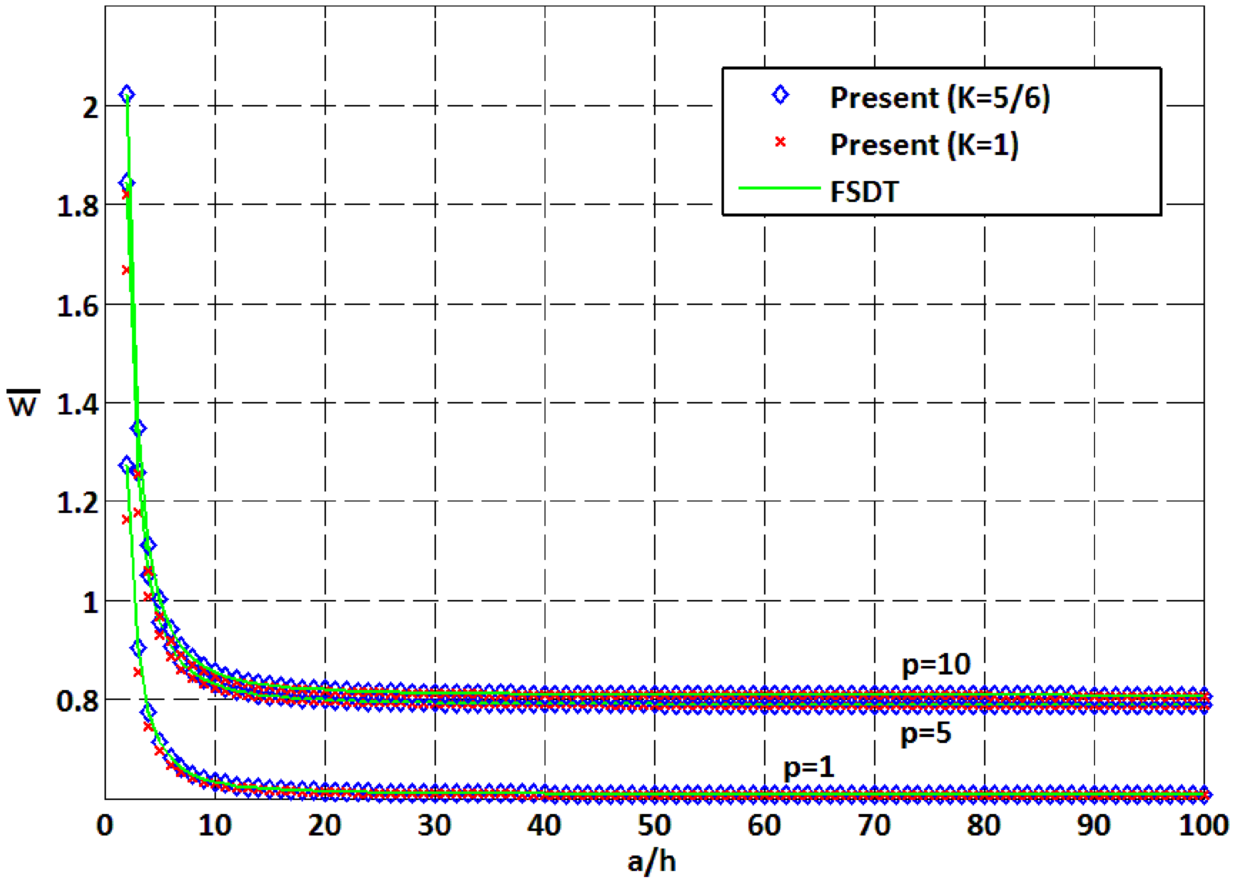

(b) Sandwich plate with an FG core and isotropic skins.

Figure 5.

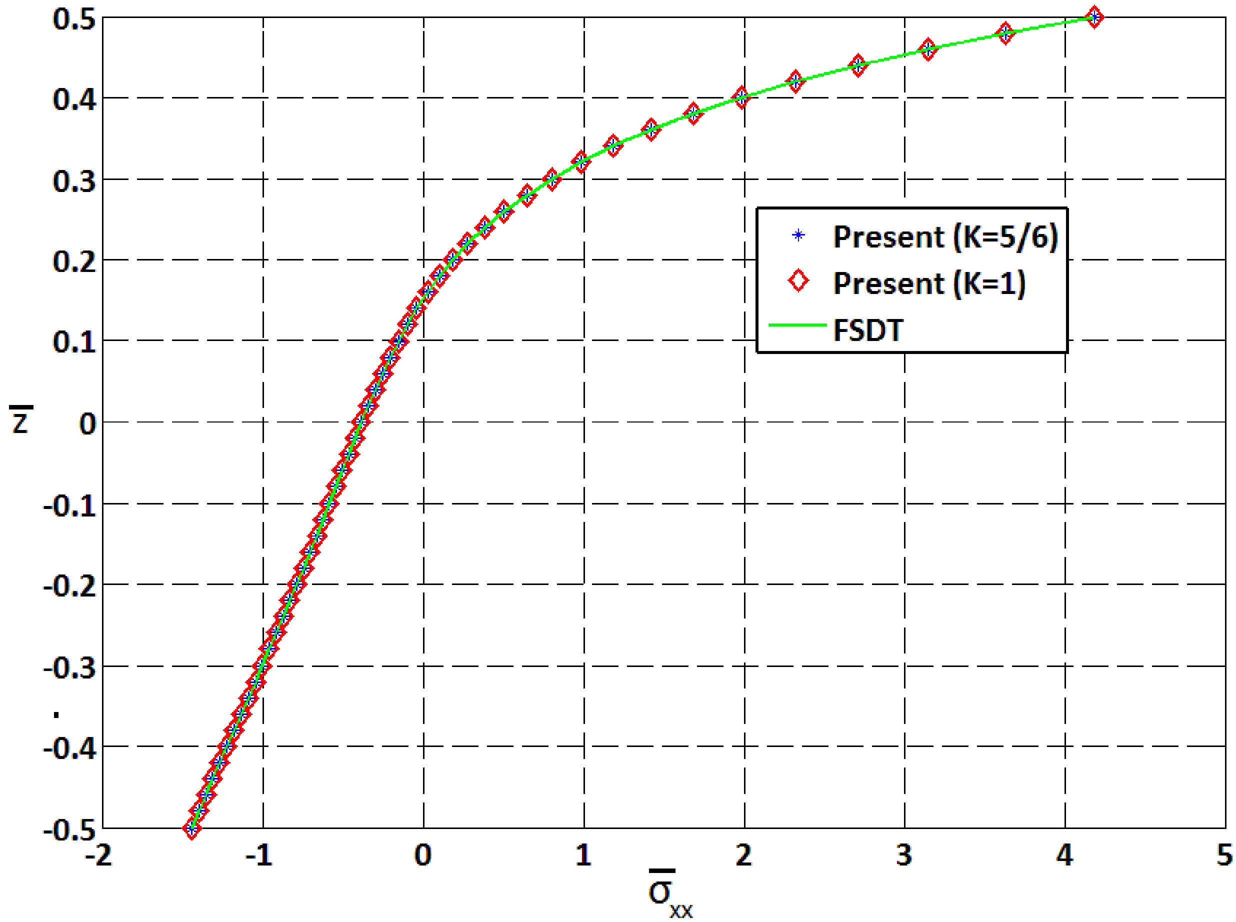

0.5
0.4
0.3
0.2
0.1
z
0
-0.1
-0.2
-0.3
-0.4
-0.5
-2
-1
0
1
2
3
4
5
σ xx
Present (K=5/6)
Present (K=1)
FSDT

(a)

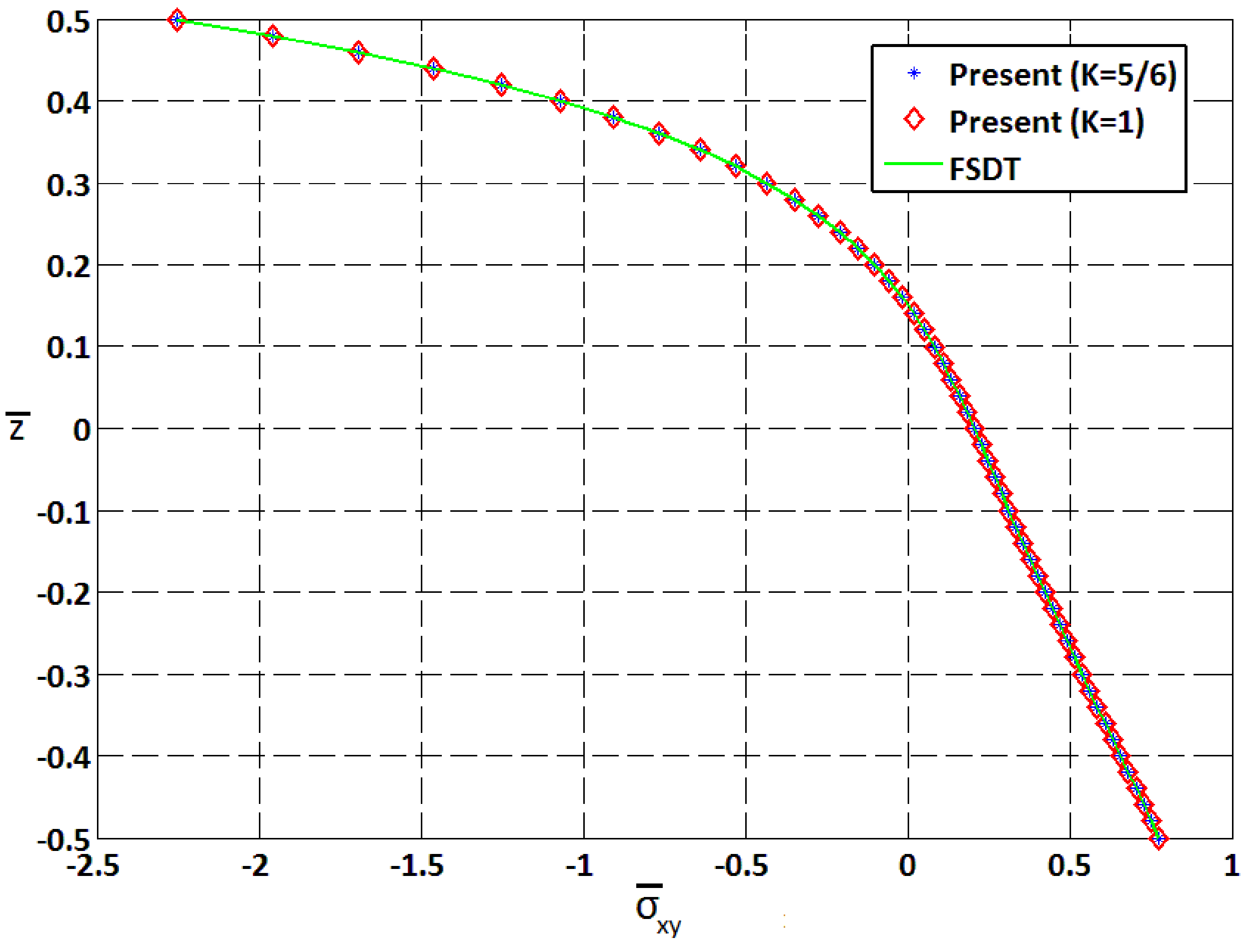

Present (K=5/6)
Present (K=1)
FSDT
0.5
0.4
0.3
0.2
0.1
0
-0.1
-0.2
-0.3
-0.4
-0.5
-2.5
-2
-1.5
-1
-0.5
0
0.5
1
$\overline{z}$
$\overline{\sigma}_{xy}$

(b)

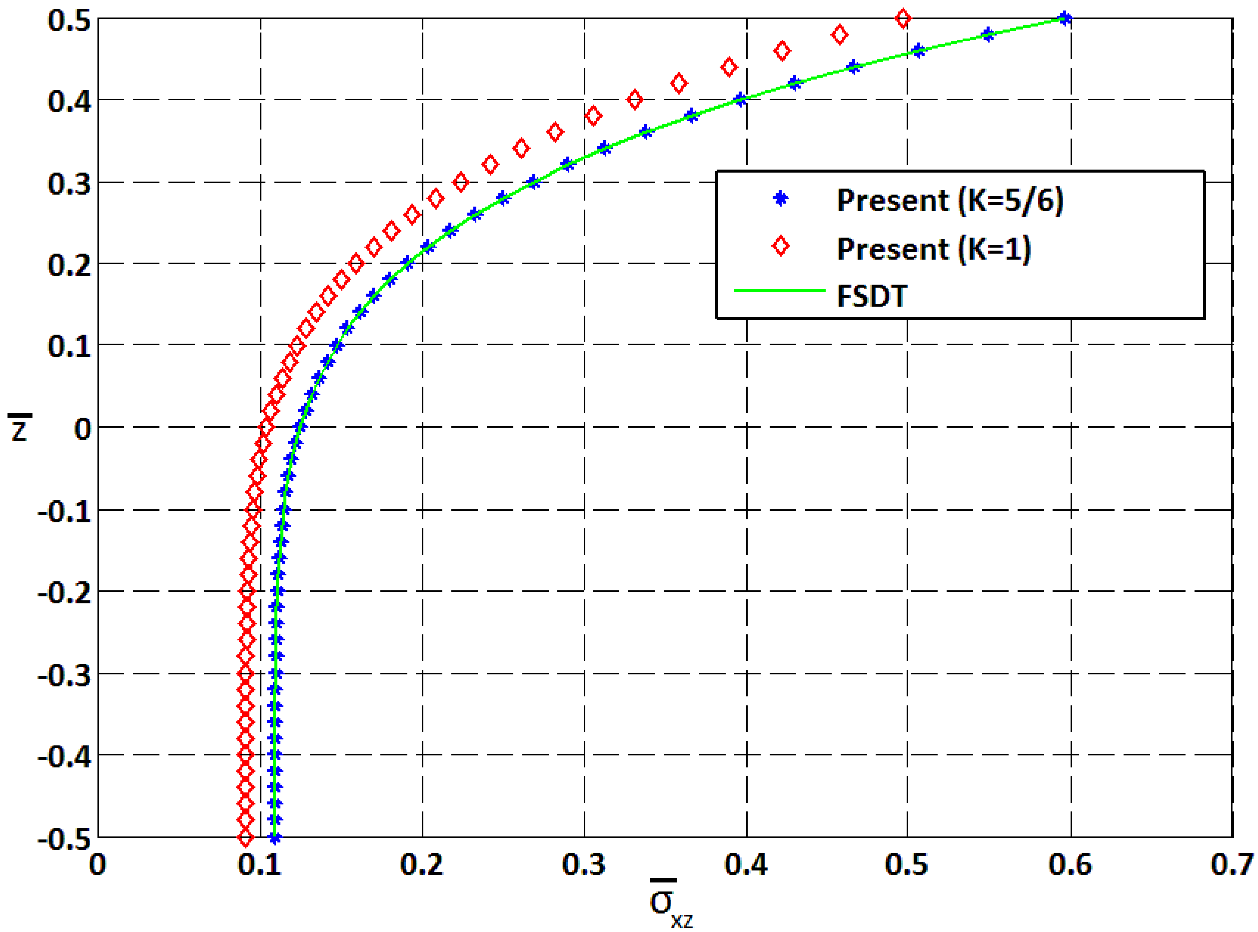

0.5
0.4
0.3
0.2
0.1
0
-0.1
-0.2
-0.3
-0.4
-0.5
z̄
0
0.1
0.2
0.3
0.4
0.5
0.6
0.7
σ̄xz
Present (K=5/6)
Present (K=1)
FSDT

(c)